2. Kratschmer, W., Lamb, L. D., Fostiropoulos, K. and Huffman, D. R., *Nature*, 1990, **347**, 354.
3. Haddon, R. C., *et al.*, *Nature*, 1991, **350**, 320.
4. Hebard, A. F., et al., Nature, 1991, **350**, 600.
5. Holczer, K. R., *et al.*, *Science*, 1991, **252**, 1154.
6. Rossiensky, M. J., *et al.*, *Phys. Rev. Lett.*, 1991, **66**, 2830.
7. Kelty, S. P., Chen, C. C. and Lieber, C. M., *Nature*, 1991, **352**, 223.
8. Chen, C. C., Kelty, S. P. and Lieber, C. M., Science, 1991, **253**, 886.
9. Tanigaki, K., *et al.*, *Nature*, 1991, **352**, 222.
10. Heiney, P. A., *et al.*, *Phys. Rev. Lett.*, 1991, **66**, 2911.
11. Stephens, P. W., *et al.*, *Nature*, 1991, **351**, 632.
12. Weaver, J. H., *et al.*, *Phys. Rev. Lett.*, 1991, **66**, 1741; Benning, P. J., Martins, J. L., Weaver, J. H., Chibante, L. P. F. and Smalley, R. E., *Science*, 1991, **252**, 1417.
13. Saito, S. and Oshiyama, A., *Phys. Rev. Lett.*, 1991, **66**, 2637.
14. Bethune, D. S., Meijer, G., Tang, W. C. and Rosen, H. J., *Chem. Phys. Lett.*, 1990, **174**, 219; Cappilletti, R. L., *et al.*, *Phys. Rev. Lett.*, 1991, **66**, 3261.
15. Prassides, K., *et al.*, *Nature*, 1991, **354**, 462; Duclos, S. J., Haddon, R. C., Glarum, S. H., Hebard, A. F. and Lyons, K. B., *Science*, 1991, **254**, 1625.
16. Holczer, K., *et al.*, *Phys. Rev. Lett.*, 1991, **67**, 271.
17. Uemera, Y. J., *et al.*, *Nature*, 1991, **352**, 605.
18. Zhang, Z., Chen, C. C., Kelty, S. P., Dai, H. and Lieber, C. H., *Nature*, 1991, **353**, 333; Zhang, Z., Chen, C. C. and Lieber, C. M., *Science*, 1991, **254**, 1619.
19. Rotter, L. D., *et al.*, *Nature*, 1992, **355**, 532.
20. Iqbal, Z., *et al.*, *Science*, 1991, **254**, 826.
21. Kortan, A. R., *et al.*, *Nature*, 1992, **355**, 529.
22. Parker, D. H., *et al.*, *J. Am. Chem. Soc.*, 1991, **113**, 7499.
23. Haufler, R. E., *et al.*, *J. Phys. Chem.*, 1990, **94**, 8634.
24. Pradeep, T. and Rao, C. N. R., *Mater. Res. Bull.*, 1991, **26**, 1101.
25. Howard, J. B., McKinnon, T., Makarovsky, Y., Lafleur, A. L. and Johnson, M. E., *Nature*, 1991, **352**, 139.
26. Arbogast, J. W., *et al.*, *J. Phys. Chem.*, 1991, **95**, 11.
27. Curl, R. F. and Smalley, R. E., *Sci. Am.*, 1991, (October), 54–63.
28. Mathews, C. K., *et al.*, *Curr. Sci.*, 1991, **61**, 834.
29. Ajie, H., *et al.*, *J. Phys. Chem.*, 1990, **84**, 8630.
30. Duclos, S. J., Haddon, R. C., Glarum, S. H., Hebard, A. F. and Lyons, K. B., *Solid State Commun.*, 1991, **80**, 481.
31. Tycko, R., *et al.*, *J. Phys. Chem.*, 1991, **95**, 518.
32. Duclos, S. J., Brister, K., Haddon, R. C., Kortan, A. R. and Thiel, F. A., *Nature*, 1991, **351**, 380.
33. Fleming, R. M., *et al.*, *Nature*, 1991, **352**, 701.
34. Zhou, O., *et al.*, *Nature*, 1991, **351**, 462.
35. Fleming, R. M., *et al.*, *Nature*, 1991, **352**, 787.
36. McCauley, Jr., J. P., et al., *J. Am. Chem. Soc.*, 1991, **113**, 8537.
37. Wang, H. H., *et al.*, *Inorg. Chem.*, 1991, **30**, 2838.
38. Benning, P. J., Martins, J. L., Weaver, J. H., Chibante, L. P. F. and Smalley, R. E., *Science*, 1991, **252**, 1417.
39. Tycko, R., *et al.*, *Science*, 1991, **253**, 884.
40. Sundar, C. S., *et al.*, *Indian J. Chem.*, 1992, (in print).
41. Guo, Y., Karasawa, N. and Goddard III, W. A., *Nature*, 1991, **351**, 464.
42. Yousuf, M., *et al.*, (under preparation).
43. Neumann, D. A., *et al.*, *Phys. Rev. Lett.*, 1991, **67**, 3808.
44. Samara, G. A., *et al.*, *Phys. Rev. Lett.*, 1991, **67**, 3136.
45. Yannoni, C. S., Johnson, R. D., Meijer, R. J., Bethune, D. S. and Salem, J. R., 1991, **95**, 9.
46. Hariharan, Y., *et al.*, Paper submitted to 'Superconductivity, Materials Physics and Applications', ICMAS-92, Houston, Texas, October 1992.

RESEARCH ARTICLE

Climatology of long-period oscillations in the equatorial middle atmosphere over Thumba, India

S. C. Chakravarty, Jayati Datta and C. P. Revankar

Indian Space Research Organisation Headquarters, Bangalore 560 094, India

The reference middle atmospheric profiles of temperature, zonal/meridional winds have been derived for two successive periods of nine years each (1971–79, 1980–88) between 20 and 80 km from the regular meteorological rocket launches over Thumba (8°32'N, 76°52'E). The analysis of long-period oscillations from the 18-years data shows that there has not been any significant change in the pattern of these oscillations and temperature structure. There are considerable intercycle/interannual variations in the periods and amplitudes of quasibiennial oscillation (QBO) and interannual and intra-annual variations of semiannual oscillation (SAO). The yearly deviations of the peak SAO amplitudes from the climatological mean value and similar deviations of the area weighted annual rainfall amount over India are positively correlated with more than 95% confidence level. Higher values of SAO amplitudes are found to be associated with the westerly phase of QBO. Using the basic mechanism of equatorial wave-mean flow interactions, the characteristics of QBO and SAO have been explained. An attempt has been made to examine the results of the intercycle/interannual/intra-annual variations of the long-period oscillations based on these theoretical considerations.

Under Indo-USSR collaboration in space research, meteorological M-100 rockets are being launched once a week, on every Wednesday evening from Thumba

(8°32'N, 76°52'E) since December 1970 for measuring pressure, temperature and horizontal wind velocities in the middle atmospheric height range of 20–80 km. As a result of this effort a long and unique meteorological data set is now available for the middle atmosphere over the equatorial region. By using different lengths of available data, sudies have been carried out to derive the mean temperature and wind profiles and their variations representative of a low-latitude station[1-4].

Using primarily the monthly average zonal wind velocities computed from the above data, a number of investigations have been carried out on the basic characteristics of stratospheric and mesospheric long-period oscillations over Thumba[5-10]. The broad features of the amplitude and phase variations of the three dominant long-period oscillations known as quasibiennial, annual and semiannual oscillations (QBO, AO and SAO) in zonal wind velocities have been derived by these authors.

In the global context of these studies, observations of both meteorological rocket-borne sensors and satellite radiometers have been utilized to study the middle atmospheric dynamical processes. While rocket data provide information on winds and temperatures, satellites are useful to obtain temperature and geopotential height fields over land and oceanic regions. Away from the equator, the satellite geopotential height gradients have been used to determine zonal and meridional winds of synoptic scale processes from the approximate balance of the pressure gradient and Coriolis forces. However, over the tropical latitudes this simplification provides erroneous data since the Coriolis force is negligible near the equator. Due to this limitation meteorological rocket data has mainly been used to study middle atmospheric wind fields over the stations located in the tropical region.

The observational data of wind and temperature fields in the middle atmosphere are generally analysed by separating these fields into longitudinally averaged zonal mean values and deviations from the zonal mean or eddies. Alternatively the fields are divided into long-term temporal averages and its deviations at different time scales. For example, the wind fields in the stratosphere and mesosphere primarily consisting of contributions from planetary-scale waves can be represented by a combination of a zonal mean flow and the eddy components of deviations from this zonal mean.

From the analysis of 10 years of rocket wind data collected over a network of stations, Hopkins[11] derived the global characteristics of the stratospheric and mesospheric circulation. The main results are the following: (a) Apart from the strong AO driven by the differential ozone heating of the upper stratosphere and the mesosphere, there is a substantial SAO with maximum easterlies near the solstices and maximum westerlies near the equinoxes. Although SAO of zonal wind component is global in nature it has maximum amplitudes near the equatorial stratopause (~ 50 km) where it dominates over the annual component. While the phase of the easterlies appear to remain steady with height, the westerlies show downward phase propagation. (b) there is a very strong QBO in the zonal wind and temperature with periods ranging between 26 and 30 months with its maximum sphere of influence in the lower stratosphere over the tropics. QBO is characterized by downward phase propagation of alternating easterly and westerly zonal wind regimes and a Gaussian distribution of maximum amplitude around the equator with a latitudinal half-width of about 12°.

Apart from the meteorological rocket soundings from Thumba mentioned earlier, Indian-made RH-200 rockets have also been launched every Wednesday from Sriharikota (13°42'N, 80°12'E) and Balasore (21°36'N, 86°56'E) for the periods 1979–80 and 1979–88 respectively. Presently M-100 and RH-200 rocket observations are being continued from Thumba and Balasore every alternate week. RH-200 rockets provide wind data between 20 and 60 km derived from radar tracking of the chaff cloud released at the apogee of the flight. The data has been extensively used to study the characteristics of the tropical middle atmospheric long-period oscillations and other related features. Nagpal *et al.*[10] have summarized the results obtained so far which broadly agree with those mentioned above and those obtained by Belmont[12] who used the data from the global network of meteorological rocket launching stations during the period 1960–82.

Since the discovery of Yanai and Maruyama[13] and Wallace and Kousky[14] about the possible excitation of Kelvin and mixed Rossby-gravity (MRG) wave modes in the equatorial atmosphere, attempts have been made to explain the evolution of QBO and SAO based on the upward propagation of these waves from the troposphere transporting eddy momentum and heat fluxes which interact with the mean zonal winds and temperature state of the stratosphere[15-17]. Although full three-dimensional models of the interaction of these upward propagating equatorial waves with the zonal mean flow and temperature structure are yet to be developed, analytical studies carried out with simple one-dimensional models have shown that the theory can account for the observed pattern of QBO quite satisfactorily[18-20]. Using β-plane approximation for these equatorially trapped waves, where the wave fields decay away from the equator, the meridionally integrated zonal average acceleration is shown to be nearly equal to the rate of change of meridionally integrated zonal eddy momentum flux. Solutions to such equations are obtained assuming single frequency modes of Kelvin and MRG waves having steady amplitudes and subject to radiative damping[16]. Based on this theory the westerly phase of

QBO and SAO and easterly phase of QBO have been evaluated. However, it has not been possible to elucidate the easterly phase of SAO on the basis of momentum transfer by vertically propagating MRG waves. Observational data has provided evidence for the existence of high-frequency Kelvin or Hirota waves in the equatorial upper stratosphere for accelerating the westerly phase of SAO[21].

Recently three equatorial wave campaign experiments have been carried out under the Indian Middle Atmosphere Programme (IMAP), using balloon and rocket-borne wind measurement at close intervals during both winter and summer. Preliminary results only have been published. Main results of these campaigns so far have been (a) upward phase propagation of 12–20 day period waves in the lower stratosphere during summer[22], and (b) in winter (Jan–Feb) there is an enhanced activity of waves with periods greater than 20 days in the troposphere and upper stratosphere/mesosphere[23]. The overall implications of these new results are yet to be assessed on the basis of theoretical understanding of their generation mechanisms, propagation and dissipation features. The results of the equatorial wave campaign mentioned above indicate that easterly momentum for SAO could result from the long-period waves which have enhanced activity in this region. However it has not been possible to confirm whether these are the horizontally propagating planetary wave modes of the middle latitudes of the winter hemisphere[23]. Further results are awaited from all the three equatorial wave campaigns carried out during IMAP.

The main purpose of this paper is to analyse the temperature, zonal wind and meridional wind profiles measured over Thumba during the 1971–88 period and derive the multiannual mean profiles of these parameters to explore any climatological shifts of middle atmospheric meteorological state during the two epochs, i.e. 1971–79 and 1980–88. Although chosen somewhat arbitrarily, these two epochs have approximately similar average solar activity conditions. The analysis is extended to study the climatological trends, intercycle/interannual and intra-annual variations of the amplitudes and phases of QBO, AO, SAO and other oscillations using the time-height series of the temperature and zonal wind data. The aspects of interannual and intra-annual variability have not been investigated in detail so far and hence these are particularly considered in this paper.

Method of analysis

Data used in the present study consist of weekly values of temperature, zonal/meridional winds available at 1 km height intervals between 20 and 80 km altitude over Thumba during the period 1971–88. Except for the relatively long data gap between 1974 and 1975, the time height series is quite consistent. Number of missing values of data (2–3 weeks at any instance) increases above 60 km and so is the relative statistical error. The weekly data is converted into monthly mean values so as to obtain 216 data points at each height. Interpolation of missing monthly means are carried out by selecting the best fit determined from visual trend of the data, polynomial spline fitting of data and the climatological average value for the particular month derived from the whole time series. The homogeneous and continuous data set so created is the basis for all analyses presented here. In order to derive the amplitudes and phases of different oscillations, the whole time series of monthly averages (216 points for each height) is converted into frequency domain by using discrete Fourier transform (DFT) function as follows[24].

$$X(k) = \sum_{n=0}^{N-1} x(n)\, W_N^{kn}$$

where $W_N = \exp(-j(2\pi/N))$, N is total number of data points and $X(k)$'s are the corresponding transformed data values in frequency scale. $X(k)$'s are obtained in complex numbers which are used to calculate the amplitudes and phases of oscillations with different periodicities. Unlike previous authors who use the method of least squares to fit the data by assuming that contributions to total zonal wind is made by the corresponding harmonic functions of QBO, AO and SAO in the above method of DFT, such assumptions are not necessary and hence there is no inherent bias to extract characteristics of oscillations with certain preferred periods. After determining the dominant modes of oscillations from DFT analysis of the entire time series, harmonic analysis with least-square fitting is used for further computations. For studying the interannual and intra-annual variations of different oscillations, contributions due to longer-period oscillations are removed before carrying out further DFT analysis on the residual time series. This is done to ensure that there is no aliasing between different modes and characteristics of each oscillation can be clearly separated. In DFT analysis, any length of time series data can be used to determine the genuine frequencies of oscillations which appear concurrently and which can be checked by cross-correlation technique involving different spectra by artificially varying the length of the time series. This method is very effective in separating the main periods of oscillations at different levels of the atmosphere.

Rocket data on winds over Balasore and Sriharikota are also available but for much shorter periods and hence these are not considered here for studies of possible changes in climatic pattern of stratospheric dynamics as the results will not be directly comparable in this context.

Results

The results of the analysis of 18 years data over Thumba related to the reference climatic profiles of temperature, zonal/meridional winds, amplitudes/phases of long-period oscillations and interannual/intercycle variations of the amplitudes of long-period oscillation are mentioned in the following sections.

Climatological reference profiles

Annual mean profiles of temperature (T), zonal winds (u) and meridional winds (v) computed separately for the two epochs, i.e 1971–79 and 1980–88 are shown in Figure 1. These profiles are considered to be representative of climatological reference model equatorial middle atmosphere. The general features seen in Figure 1 are: (a) Temperature maximum occurs around 47 km altitude primarily due to the heating produced through absorption of solar UV radiation by ozone. (b) There is an increase in temperature of about 7°C between 50 and 70 km altitudes during the 1980–88 epoch compared to that for the period 1971–79. The difference between the average sunspot numbers, although quite small (~ 20), could probably account for this increase in temperature due to additional solar UV fluxes which is known to vary substantially with solar activity. (c) The corresponding zonal wind profile shows a predominantly easterly circulation in the stratosphere and westerly circulation in the mesosphere which is in conformity with the global mean circulation pattern. (d) The amplitudes of mean meridional winds are about an order of magnitude less than the amplitudes of zonal winds up to the stratopause, thereafter the meridional circulation increases in the upper mesosphere quite significantly. The multiannual climatological reference amplitudes of T, u and v with respect to the entire period 1971–88 are given in Table 1 with corresponding standard errors at three sigma level.

Long period oscillations

Using the 216 monthly mean values, the DFT analysis has been carried out separately for the two epochs as well as for the entire period. As an illustration the frequency spectra at 47 km from the three time series are shown in Figure 2. It is seen that the periods for the corresponding frequencies which match exactly in both the series in Figure 2, *a* correspond to AO, SAO and TAO (terannual oscillation). Although the amplitude of QBO at this height is small, a clear shift in the periods of QBO is indicated between the two epochs. During the first half (1971–79) QBO has a period of 28 months whereas for the second half (1980–88) it is 32 months. This feature of an increase in average period of QBO for the second epoch is verified by similar DFT spectra

Table 1. Climatological reference middle atmospheric temperature, zonal wind and meridional winds over Thumba (1971–88)

Height (km)	Temperature (K)	Zonal wind (m/s)	Meridional wind (m/s)
80	194.3 ± 2.7	-3.7 ± 8.1	2.2 ± 5.4
70	199.7 ± 1.2	14.7 ± 4.8	-2.2 ± 2.7
60	233.4 ± 1.2	10.4 ± 2.7	-3.1 ± 1.5
50	262.9 ± 0.6	4.8 ± 2.7	0.9 ± 1.8
40	255.8 ± 0.6	-10.3 ± 1.8	-0.6 ± 0.9
30	232.1 ± 0.4	-16.2 ± 1.8	-1.2 ± 0.6
20	204.0 ± 1.5	-4.2 ± 2.1	-0.3 ± 0.9

Standard errors are shown at 3σ level.

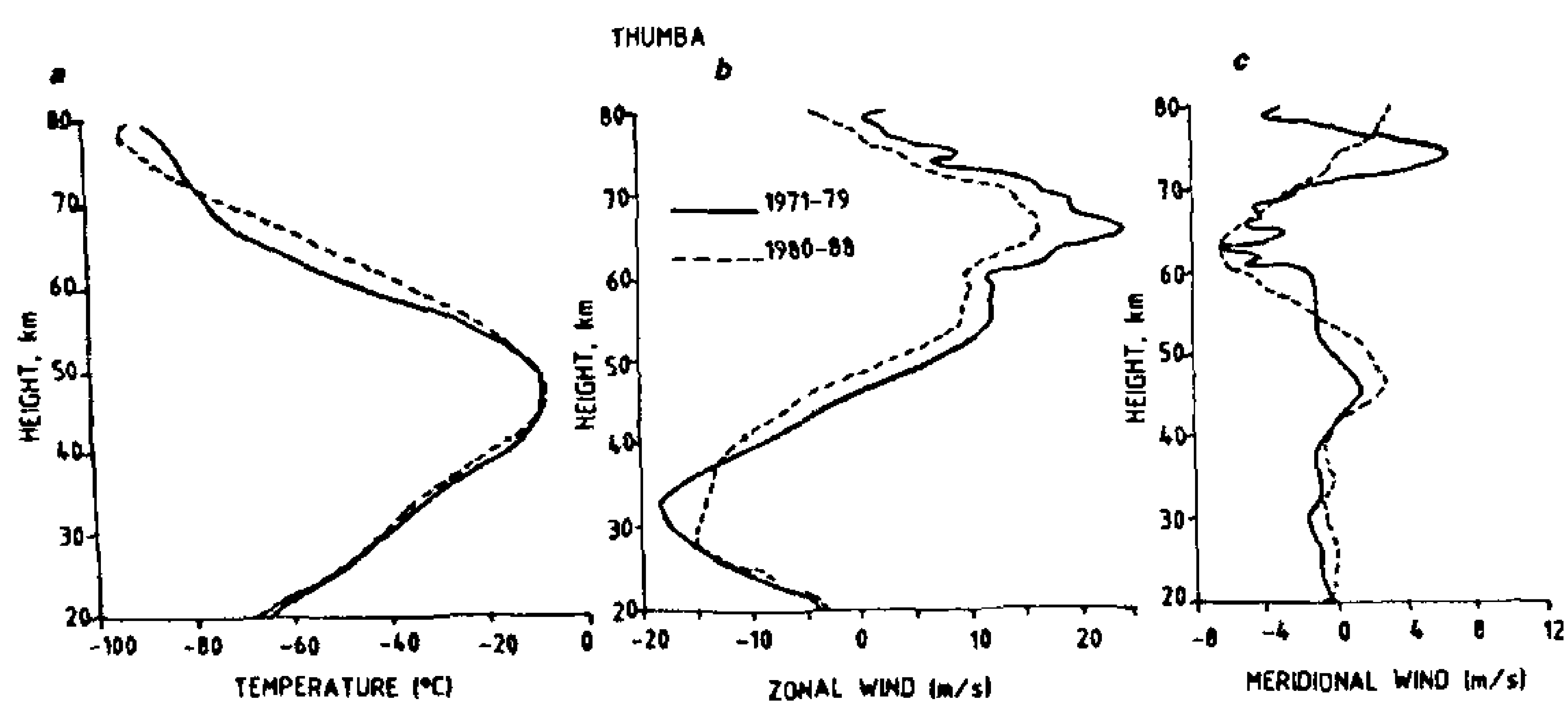

Figure 1. Mean profiles of (*a*) temperature, (*b*) zonal wind and (*c*) meridional wind for two epochs 1971–79 and 1980–88 over Thumba.

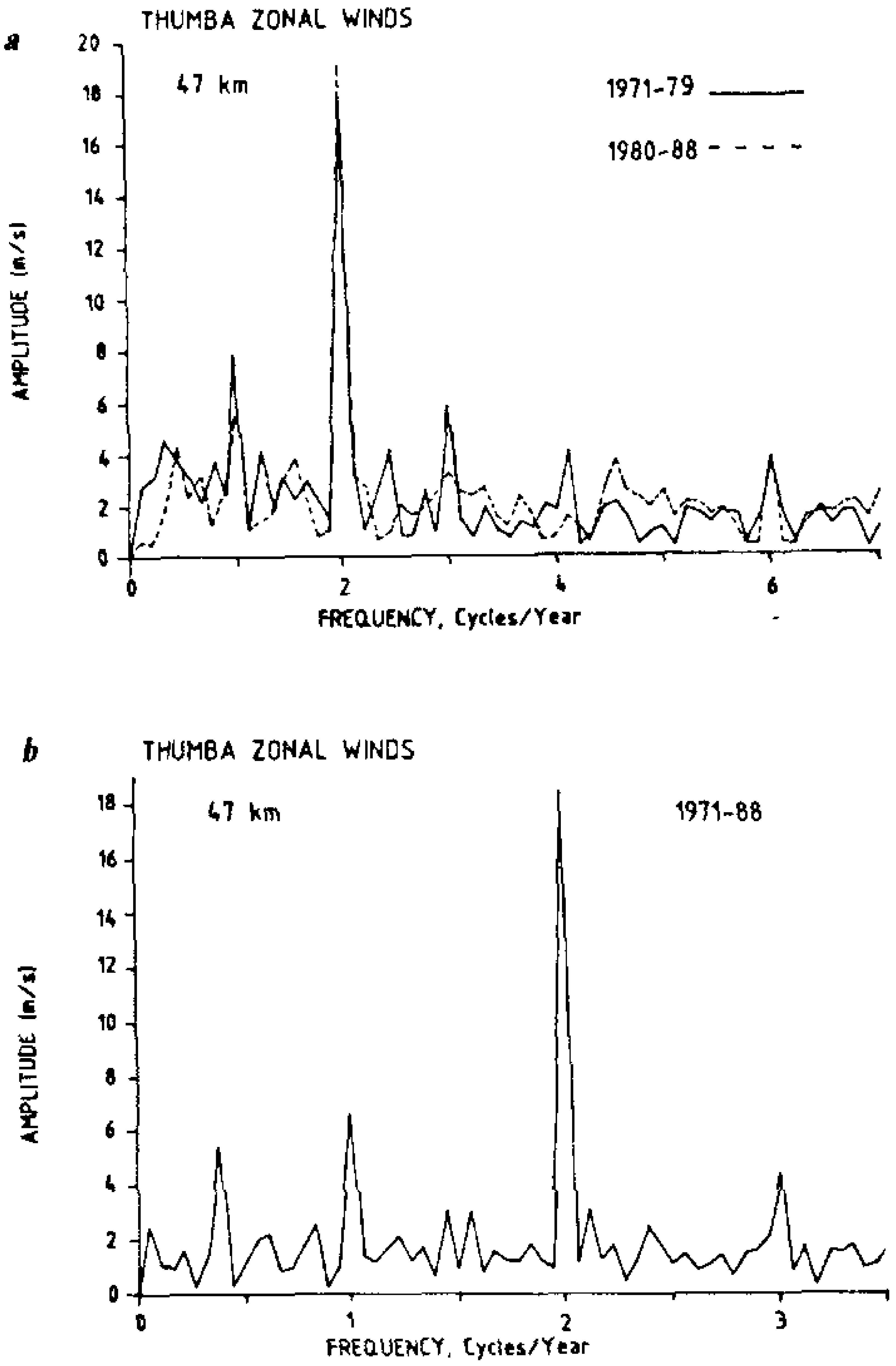

Figure 2. Discrete Fourier transform (DFT) frequency spectra for zonal winds at 47 km shown separately for (*a*) two epochs 1971–79 and 1980–88, and (*b*) the entire time series during 1971–88 over Thumba.

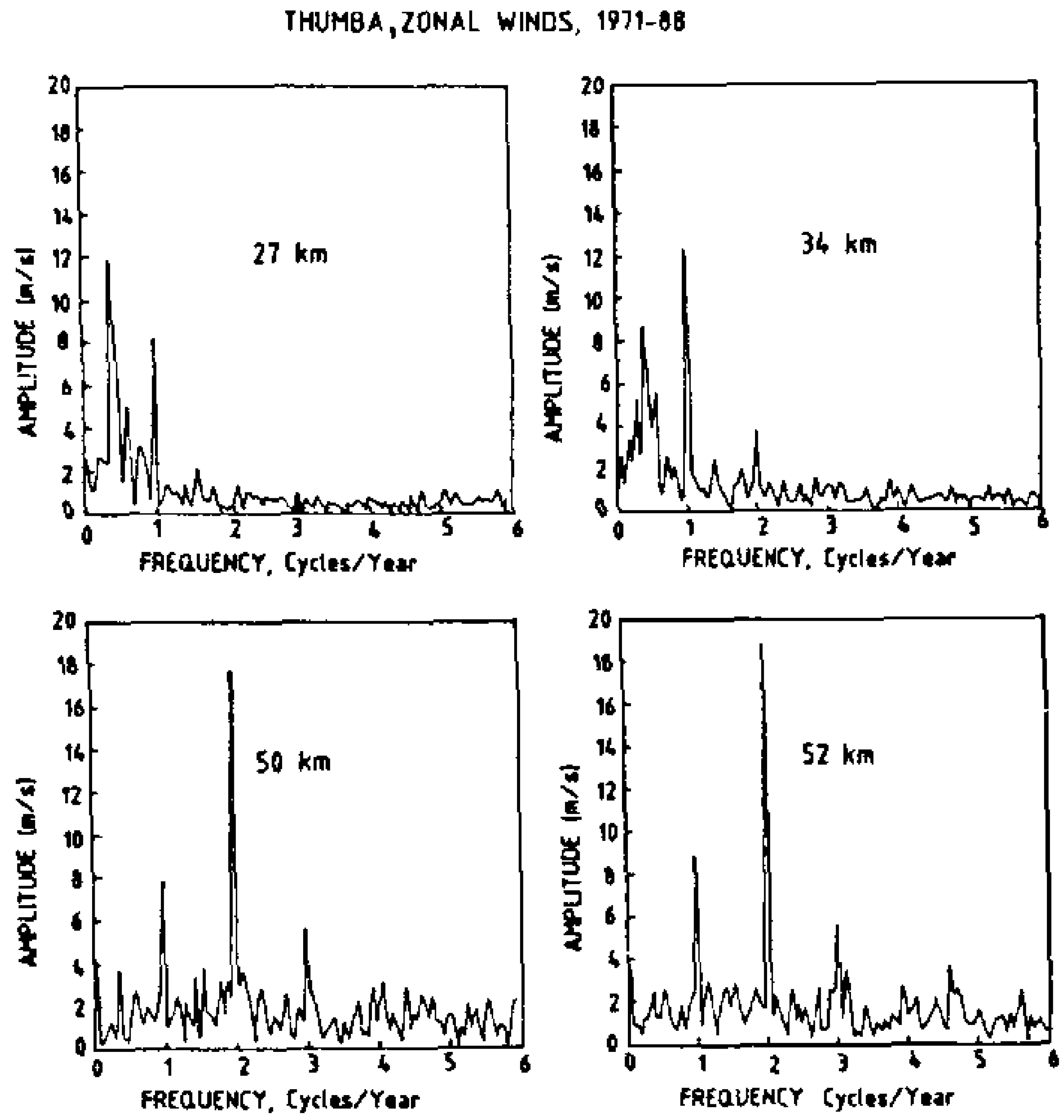

Figure 3. DFT frequency spectra for zonal winds at 27, 34, 50 and 52 km heights for the entire time series during 1971–88 over Thumba.

at other heights including the lower stratospheric heights where QBO is dominant. It can also be seen that although there are other periodicities of amplitudes less than 4 m/s these are not considered significant since the spectral peaks do not occur concurrently in the two spectra of Figure 2, *a*. By scanning these spectra at each 1 km height interval it is found that the genuine long-period oscillations consist of QBO, AO, SAO and TAO only and other oscillations are not significant as these are immersed within the inherent noise levels. While the amplitudes of TAO are relatively small they appear consistently and concurrently in the two time domains particularly at upper stratospheric and lower mesospheric regions. It can be seen from Figure 2, *b* that these dominant oscillations stand out clearly amongst others with amplitudes near the averages of corresponding amplitudes for the two separate epochs. Figure 3 shows similar power spectra of zonal winds for the whole length of data of 216 months at selected heights of 27,34,50 and 52 km. While at 27 and 34 km heights the dominant oscillations are QBO and AO, at higher altitudes of 50 and 52 km the peak amplitudes of SAO and TAO are observed respectively. From such DFT spectra at different heights, it is found that the maximum power of QBO lies between the periods of 28 and 32 months.

Derived on the basis of harmonic analysis with least-square fitting, the height profiles of the amplitudes and phases of QBO, AO, SAO and TAO for the entire period of 18 years (1971–88) are shown in Figure 4, and for the two epochs separately in Figure 5. The phase of QBO shows a downward propagation at the rate of about 1 km/month with the peak amplitude of 12 m/s occurring around 27 km. The downward phase propagation characteristic of QBO is clearly seen separately for the two epochs also but the peak amplitudes are of the order of 15 m/s. The relatively lower amplitude of 12 m/s for the climatological reference QBO is due to the averaging of different QBO cycles with varying periods of 28-32 months. The average period of QBO based on best least-square fitting for the entire period is found to be 30 months. The average periods of QBO are found to be about 28 and 32 months respectively for the two epochs, which confirms the results obtained from DFT analysis mentioned earlier.

Apart from QBO the most prominent amongst other oscillations is SAO with peak amplitudes of about 20 m/s around 50 km. The phase of SAO shows a systematic downward propagation of about 10 km/month

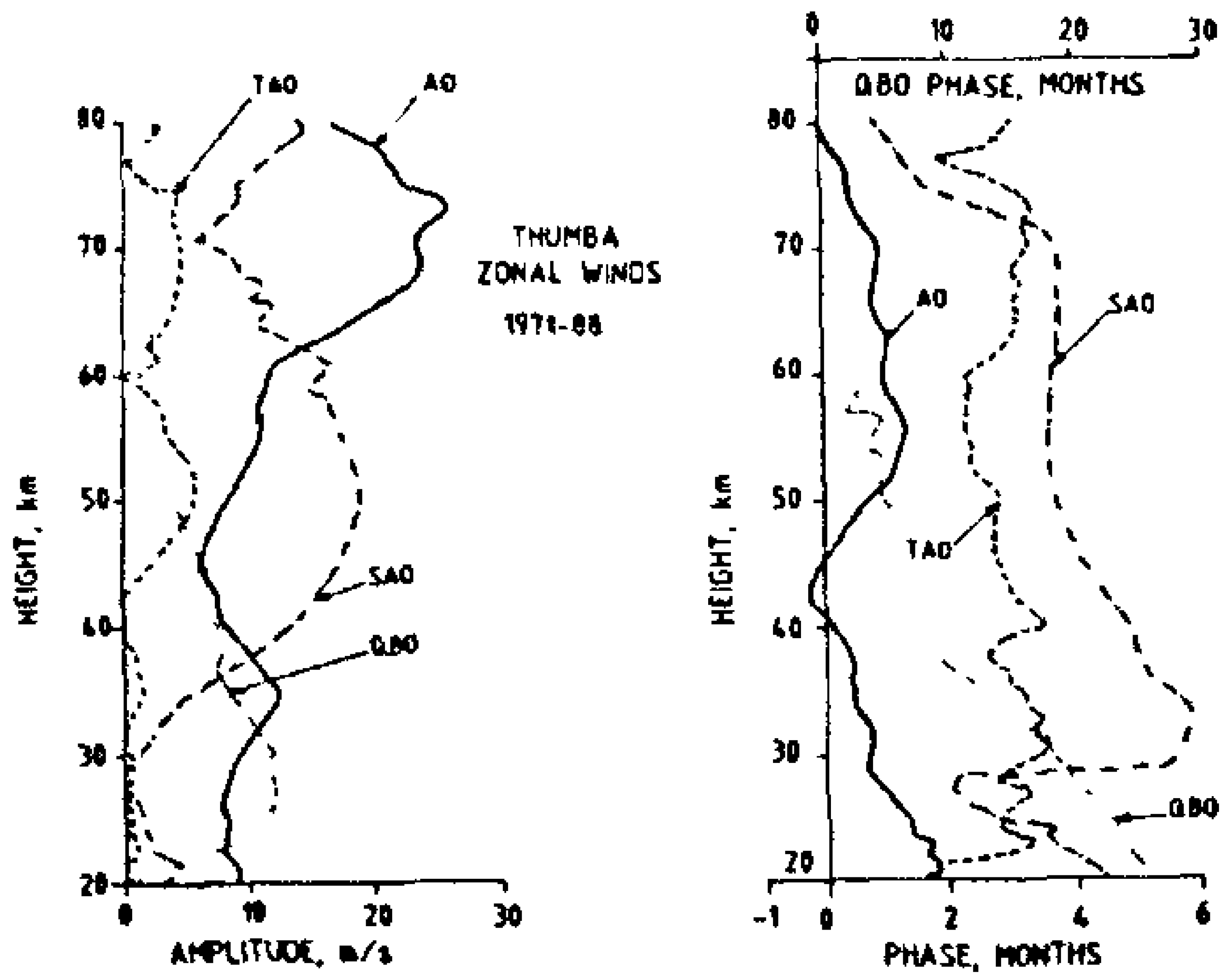

Figure 4. Height profiles of amplitudes and phases of QBO, AO, SAO, TAO in monthly mean zonal wind data for the period 1971–88 over Thumba derived by using harmonic analysis-least square fitting technique.

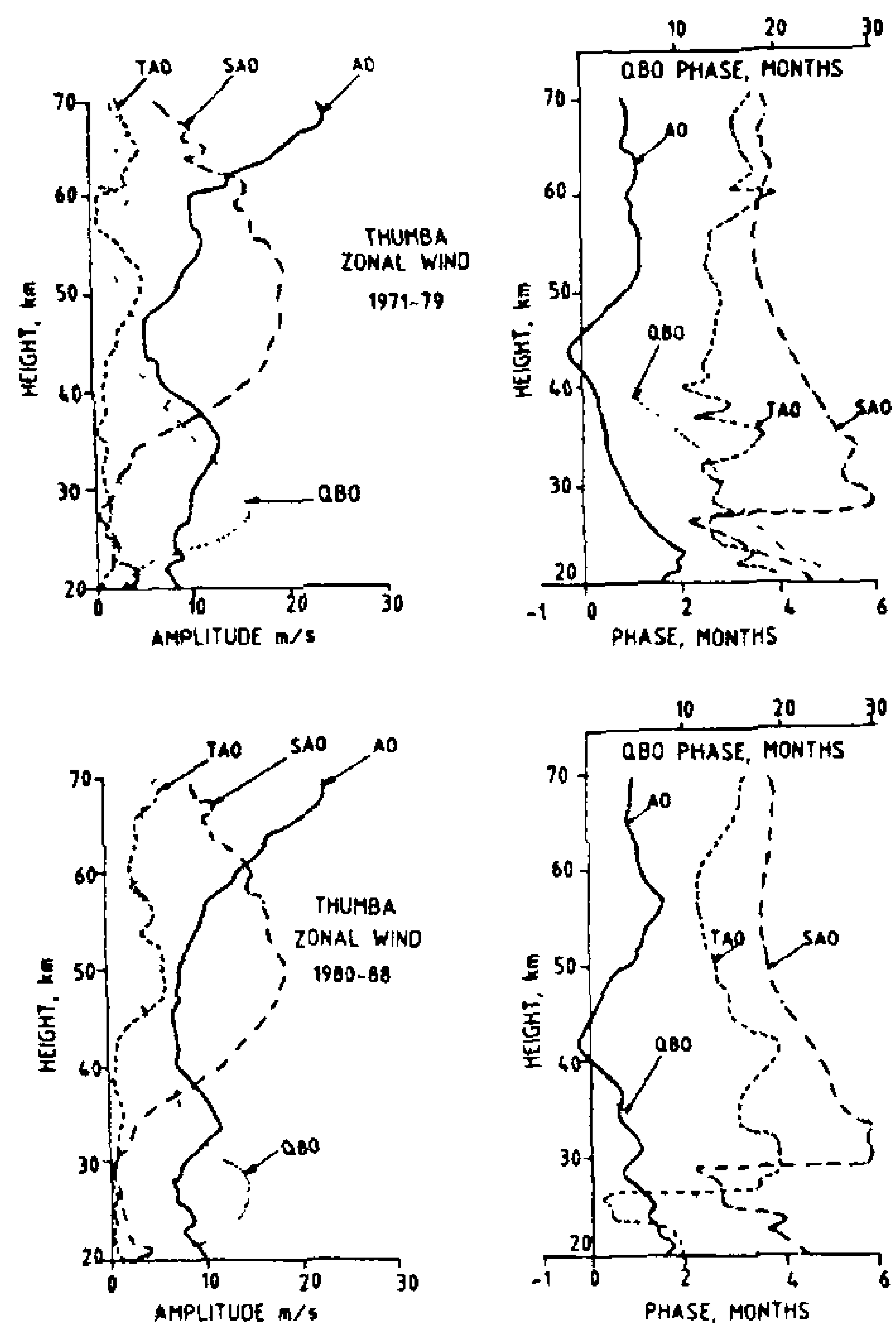

Figure 5. Same as Figure 4 but separately for two epochs 1971–79 and 1980–88.

between 50 and 35 km and appears to be steady above 50 km. There is no significant variation in the average trend of SAO amplitude profile and phase propagation for the two epochs. This indicates that there has not been any change in the average SAO characteristic over time scales of past two decades. In addition to the dominant QBO and SAO, significant AO and TAO are present below 60 km with peak amplitudes occurring around 35 km and 50 km respectively. The stratospheric annual oscillation which is weaker compared to the amplitude of the AO at mesospheric altitudes shows a downward phase propagation of about 10 km/month between 40 and 20 km. The AO phase above 40 km shows an upward propagation up to about 55 km. The downward phase variation of TAO is of the order of 1 month between 60 to 40 km, hence is considered to be stationary. In summary, the phase of all oscillations with significant peak amplitudes below 60 km show either downward propagation or invariant phase and there is no marked climatological change in the average amplitudes and phases of these long-period oscillations.

Figure 6 shows the results of similar harmonic analysis of the entire time series for temperature data. It can be seen from the figure that the prominent QBO and SAO peak amplitudes in temperature occur around 37 and 39 km and their phases show downward propagation comparable in magnitude of the corresponding values of zonal winds. There is a secondary QBO peak above 60 km with no distinct propagation in this region. Around 45 km AO shows a small peak in amplitude with downward phase propagation at a higher rate compared to the AO in zonal winds observed in the stratosphere. Considering the two epochs separately the average characteristics of these long-period oscillations in temperature fields (not shown in figure) have also remained unchanged.

Interannual and intra-annual variations of long-period oscillations

The variability in the period of QBO from one cycle to another has already been mentioned in the previous section and the results described so far dealt with average climatological trends of AO, SAO and TAO. In order to have a detailed understanding of the intercycle/interannual variation of QBO and AO and interannual/intra-annual variations of SAO and TAO, the time series is treated as mentioned in section on methods. Yearly average values of zonal winds at 27 km plotted for all the 18 years are shown in Figure 7. It can be seen that the QBO periods go through a cyclic pattern and the annual average amplitudes of the easterly phase of QBO are larger than the amplitudes of its westerly phase. There is considerable variation in the amplitudes of QBO from one cycle to the other.

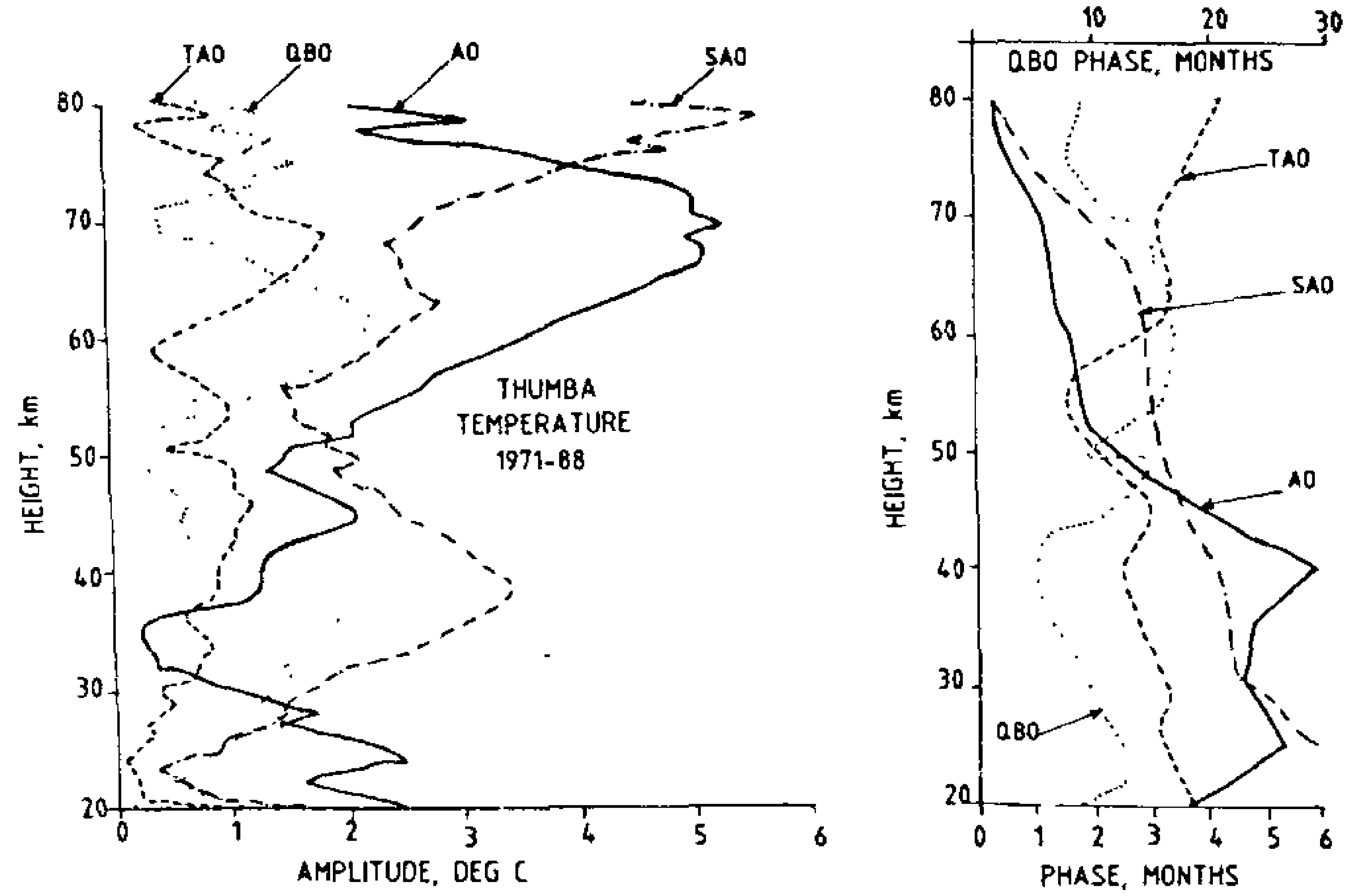

Figure 6. Height profiles of amplitudes and phases of QBO, AO, SAO and TAO in temperature data for the period 1971–88 over Thumba derived by using harmonic analysis-least square fitting technique.

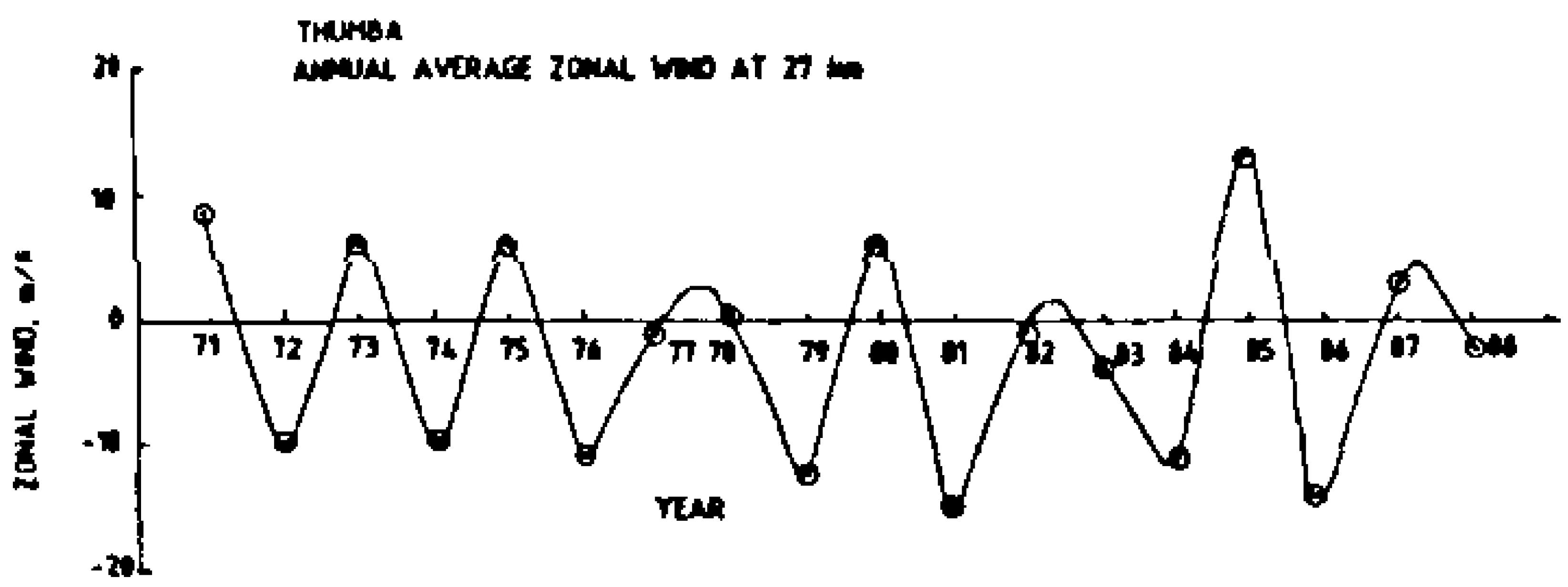

Figure 7. Yearly average values of zonal winds at 27 km during the period 1971–88 over Thumba.

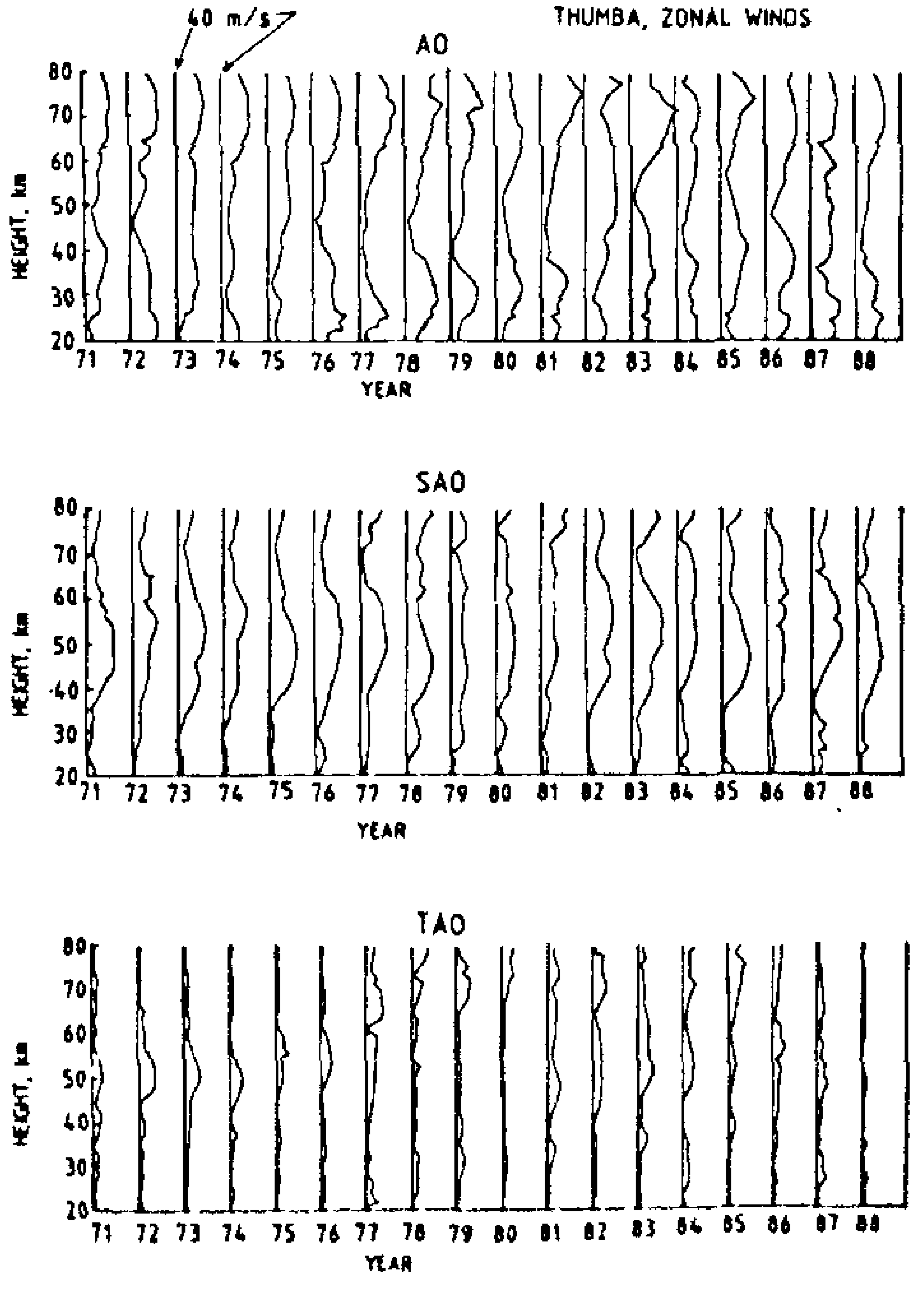

Figure 8. Height profiles of the annual amplitudes of AO, SAO and TAO for different years during 1971–88 over Thumba.

Similarly the time-height profiles of annual average amplitudes shown in Figure 8 bring out the presence of large year-to-year variations in the peak altitude and amplitudes of AO, SAO and TAO. The annual amplitudes of SAO are made up from the two full cycles of SAO within a year. The reconstructed amplitudes of the two cycles of SAO separately averaged over the entire span of 18 years are shown in Figure 9. For comparison with such a climatological reference which shows no significant intra-annual variation, the two reconstructed SAOs for an individual year 1972 are also shown in the figure. The contrast is very clear with large difference between the peak amplitudes of the two subannual SAO cycles during 1972. A scrutiny of the amplitudes of SAOs revealed that in certain years the magnitude of the two half-yearly amplitudes vary dramatically.

From the downward phase propagation of QBO and SAO, it is clear that the sources for these oscillations must reside in the troposphere. The intercyclic and

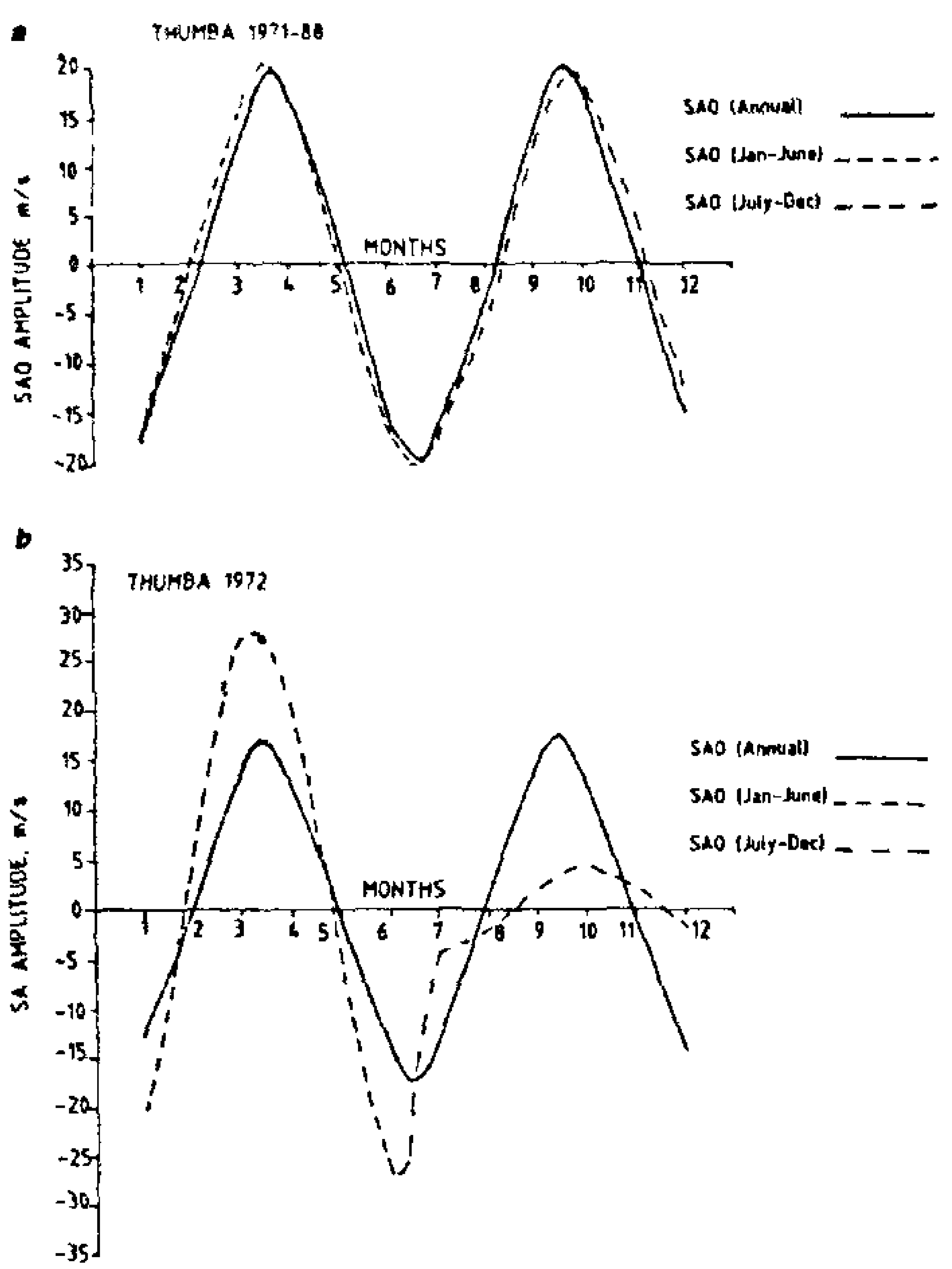

Figure 9. Reconstructed amplitudes of SAO over Thumba for (a) average annual and half-yearly cycles over the period 1971–88 and (b) same for the year 1972.

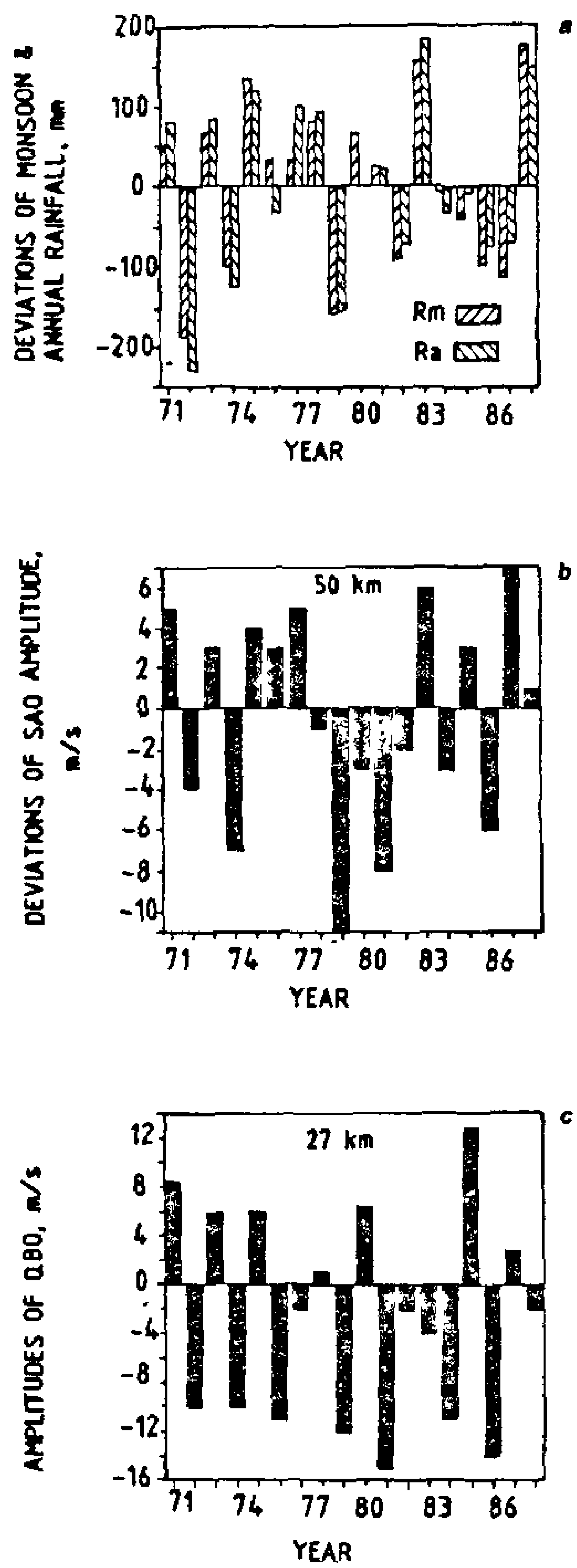

Figure 10. Deviations of (a) south-west monsoon and annual rainfall amounts over India and (b) annual average SAO amplitude at 50 km over Thumba from the corresponding climatological mean values, and (c) annual amplitudes of QBO at 27 km over Thumba.

interseasonal variation in the QBO and SAO amplitudes indicate that such tropospheric sources must be highly variable. Houze[25] has demonstrated that the magnitude of the equatorial wave forcing is governed by latent heat releases of large-scale convective phenomena and cloud clusters. Model studies by Chang[26] and Holton[27,28] have shown that randomly distributed cloud clusters and typical equatorial convective processes can generate Kelvin and MRG waves. Hence for further analysis of the source functions of the equatorial waves (which in turn influence the generation of QBO and SAO), the only parameter which can be used is the quantity of rainfall known to be related to the latent heat release in the tropospheric convective phenomena and cloud physical processes. The area weighted total SW monsoon (seasonal rainfall during June–September) and the total rainfall over Indian subcontinent have been archived for a long period. The deviations of these two rainfall parameters from their climatological average values for the period 1972–88 along with the annual amplitudes of easterly or westerly phase of QBO at 27 km and deviations of average annual SAO amplitudes at 50 km altitude are shown in Figure 10. It can be seen that on an average the years having low rainfall amount are associated with the easterly phase of QBO and below average annual amplitudes of SAO. It is to be noted that the absolute values of annual QBO phase instead of their deviations have been used here because the variability of QBO period from cycle to cycle would make deviations of QBO phase a less meaningful parameter.

Further the scatter diagram in Figure 11 shows a

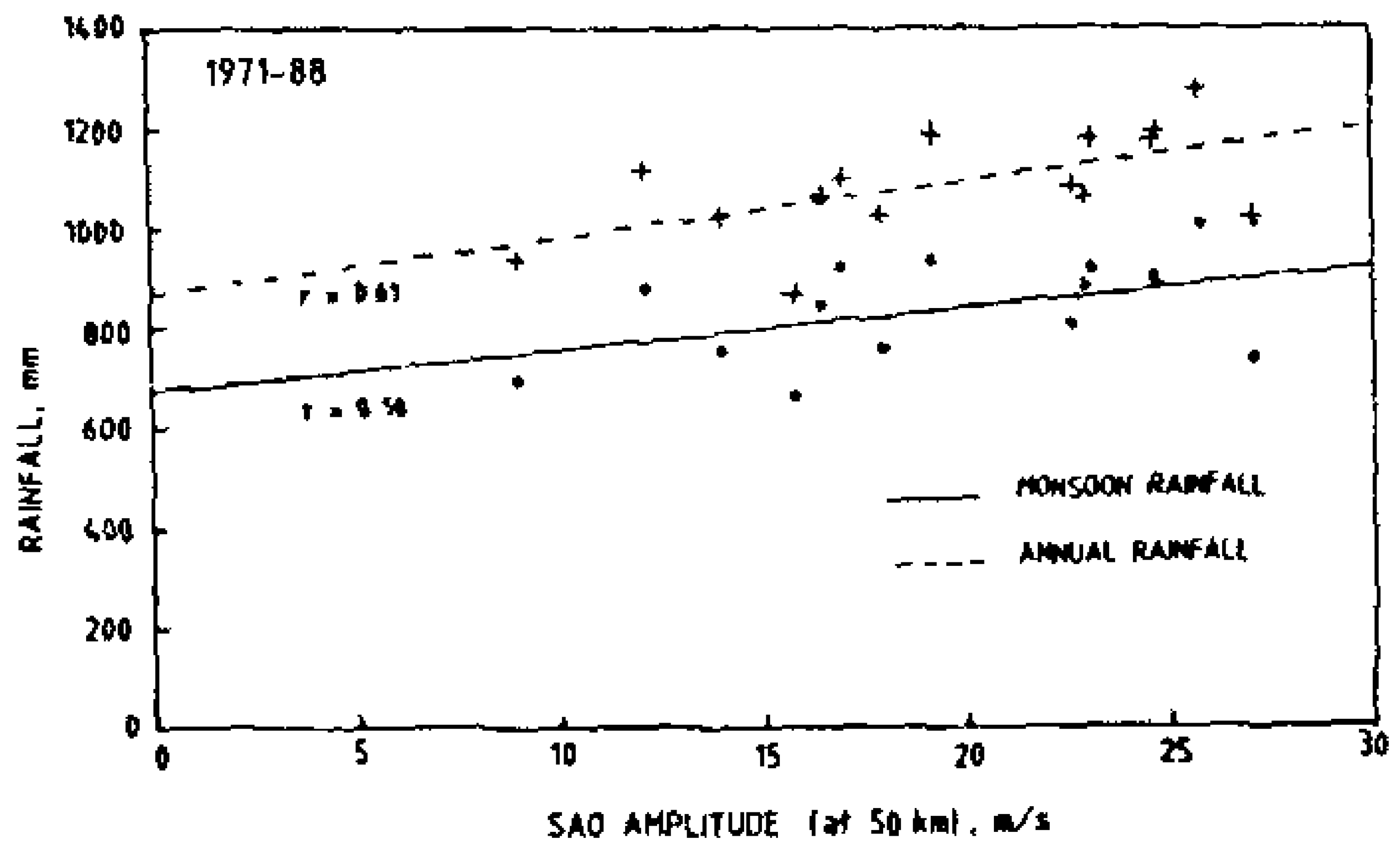

Figure 11. Scatter diagram of south-west monsoon and annual rainfall amounts over India with respect to annual SAO amplitudes at 50 km during different years of 1971–88 period. The data points for the years 1974, 1975 and 1988 which involve considerable interpolation have not been used in the scatter diagram and in deriving the correlation coefficients shown in the figure.

linear trend between the SW monsoon and total annual rainfall with the annual amplitudes of SAO at 50 km. A positive correlation coefficient of 0.61 (at 95% confidence level) between the annual rainfall amount and annual average SAO amplitude has been found establishing relationship between the tropospheric and stratospheric coupling phenomena. The correlation coefficient for SW monsoon rainfall is only 0.5 and comparatively less significant. A number of other such correlation coefficients were computed using amplitudes of different seasonal cycles of SAO and TAO but none of these were found to be significant below 5% level.

Discussion

The results presented here deal with the climatology of the thermal structure and dynamical state of the equatorial middle atmosphere. Apart from delineating the general characteristics of the well-known QBO, SAO and AO, significant magnitudes of TAO are also found to be present around 50 km altitude. Large intercycle variations, particularly in the amplitudes of QBO and SAO have been found to exist even though the climatological trends of these variations have remained unchanged in the past two decades. The interannual variations of the amplitudes of QBO and SAO are shown to be related in such a way that the strong westerly phase of QBO is associated with a higher annual average SAO amplitude. During such a year, the annual average rainfall over India has also been above the mean value. While this result is supported by earlier studies to find correlations between QBO phase and stratospheric circulation index (SCI) with rainfall during summer monsoon season over India[29,30], the association of the variability of rainfall leading to changes in QBO amplitudes and concomitant change in annual amplitudes of SAO is clearly demonstrated in this paper.

Except for TAO and the mesospheric AO, all the long-period oscillations show clear downward phase propagation which indicates the definite role played by vertically propagating equatorial wave modes in producing these oscillations. Recent theoretical/modelling studies have shown that the characteristics of these oscillations can be explained by considering the zonal wind accelerations as a result of the wave-mean flow interactions[27].

The observed QBO and its downward phase propagation have been successfully explained based on the interaction of upward propagating Kelvin and MRG waves dissipating momentum fluxes to accelerate the mean flow. Detailed theory to explain the variations of the QBO period between 28 and 32 months as well as its amplitude variation from cycle to cycle have not been developed. The state of the zonal mean flow or the prevailing winds in the upper troposphere as well as the growth and decay of random convective and cloud structures seem to play important roles in modulating QBO and SAO amplitudes. This is indicated by the results presented here. The easterly (westerly) zonal winds in the upper troposphere are transparent to the propagation of Kelvin (MRG) waves leading to their dissipation in the westerly (easterly) shear zones. While this can generate the observed characteristics of QBO, the alternating westerly (easterly) momentum transfer to mean flow would also depend on the viscous drag coefficients of the atmosphere and the relative strengths of Kelvin and MRG waves.

Taking the results of QBO and SAO together, it can be seen that both Kelvin and Hirota waves[21] may find suitable easterlies in the middle/upper troposphere to propagate upwards. While the Kelvin waves get dissipated in the easterly shear zone producing QBO's westerly phase, the Hirota waves propagate up and are thermally damped in the upper stratosphere, producing the westerly phase of SAO. Hence the resultant values of SAO westerly amplitude depend on two factors : (a) time scale development of westerly acceleration for QBO and (b) tropospheric magnitudes of the momentum fluxes which depend on the convective processes and distribution of cloud clusters in the equatorial region. During the easterly phase of QBO the propagation of Hirota waves are restricted thus inhibiting the growth of the westerly amplitude of SAO. This happens because the easterly phase of QBO is produced through the propagation and dissipation of MRG waves when the Kelvin or Hirota waves are blocked by lower-level westerlies. This relatively simple qualitative physical mechanism seems to explain the correlation between the amplitudes of SAO, zonal wind velocities of westerly phase of QBO and the rainfall characteristics. However, a detailed analytical study needs to be conducted to derive the parameters quantitatively.

Conclusions

The main conclusions of the paper are summarized below:

(i) Reference climatological models for temperature, zonal, meridional wind profiles between 20 and 80 km over Thumba (8.5°N) show that there has not been any major change in the characteristic pattern during two successive periods of nine years each, starting from 1971. Based on the entire data for 18 years the derived reference profiles for these parameters represent accurate climatological standards as compared to those obtained by earlier authors.

(ii) Both from DFT as well as harmonic analysis with least-squares fitting, it is found that the zonal wind and temperature values are mainly influenced by QBO, AO, SAO and TAO with varying amplitudes at different heights. The power spectra of zonal winds for the entire period of 18 years data indicate the presence of peak amplitudes of these oscillations at 27, 34, 50 and 52 km respectively. It is also found that there has not been any significant shift in the average characteristics of these oscillations during the two epochs mentioned above except for the period of QBO cycle which has varied from 28 months to 32 months between the two blocks of years.

(iii) While the phase variation of QBO shows a clear downward propagation at the rate of 1 km/month between 20 and 40 km, the phase variation of SAO is about 10 km/month between 35 and 55 km height range. TAO shows almost a steady phase in the upper stratosphere and lower mesosphere. The amplitude profile of AO shows two peaks one around 35 km and the other in the mesosphere (~70 km) with a downward phase propagation of about 10 km/month between 20 and 40 km altitude.

(iv) Although on a climatological scale of 18 years the trend of basic amplitude and phase variations of long-period oscillations has not changed, there have been very large intercycle variations in the amplitudes of these oscillations, particularly for QBO and SAO. Years having lower than average rainfall over India are seen to be positively correlated to the lower than average annual amplitudes of SAO and vice versa and the years of lower SAO amplitude occur when the QBO is in its easterly phase. A positive correlation of about 0.6 has been found between the deviation of the peak amplitude of SAO with respect to climatological mean and the area weighted annual rainfall over India at more than 95% confidence level. This correlation between the amplitudes of QBO, SAO and precipitation arises due to the link provided by the equatorial Kelvin/Hirota and MRG waves generated in the middle/upper troposphere and propagating into the middle atmosphere thereby interacting and influencing the mean wind fields in this region.

1. Appu, K. S., Narayanan, V., Boutko, A. I. and Koshelkov, Yu. P., Proceedings of the Central Aerological Observatory, 1981, **145**, 48.
2. Ananthasayanam, M. R. and Narasimha, R., MAP Handbook, 1985, **16**, 197.
3. Koshelkov, Yu. P., Kovshova, E. N. and Boutko, A. I., Presented at First Workshop on Scientific Results under ISRO-SCHCNE (USSR) collaboration in space meteorology and aeronomy, Bangalore, May 26–27, 1987.
4. Jain, A. R., Nagpal, O. P., Dhaka, S K. and Mathew, V., *Indian J. Radio Space Phys.*, 1989, **18**, 224.
5. Raja Rao, K. S., Thapliyal, V. and Patil, S. R., *Indian J. Radio Space Phys.*, 1975, **4**, 328.
6. Reddy, C. A. and Raghava Reddi, C., *J. Atmos. Terr. Phys.*, 1986, **48**, 1085.
7. Reddy, C. A., Raghava Reddi, C. and Mohankumar, K. G., *Quart. J. R. Meteorol. Soc.*, 1986, **112**, 811.
8. Kumar, S. and Nagpal, O. P., *Indian J. Radio Space Phys.*, 1987, **16**, 390.
9. Nagpal, O. P., *Indian J. Radio Space Phys.*, 1988, **17**, 232.
10. Nagpal, O. P., Jain, A. R. and Dhaka, S. K., *Indian J. Radio Space Phys.*, 1989, **18**, 233.
11. Hopkins, R. M., *J. Atmos. Sci.*, 1975, **32**, 712.
12. Belmont, A. D., MAP Handbook, 1985, **16**, 164.
13. Yanai, M. and Maruyama, T., *J. Meteorol. Soc. Jpn*, 1966, **44**, 291.
14. Wallace, J. M. and Kousky, V. E., *J. Atmos. Sci.*, 1968, **25**, 900.
15. Lindzen, R. S. and Holton, J. R., *J. Atmos. Sci.*, 1968, **25**, 1095.
16. Holton, J. R. and Lindzen, R. S., *J. Atmos. Sci.*, 1972, **29**, 1076.
17. Dunkerton, T., *J. Atmos. Sci.*, 1979, **36**, 32.
18. Holton, J. R., *J. Atmos Sci.*, 1974, **31**, 942.
19. Andrews, D. G. and McIntyre, M. E., *J. Atmos. Sci.*, 1976, **33**, 2031.
20. Boyd, J. P., *J. Atmos. Sci.*, 1976, **33**, 2285.
21. Hirota, I., *J. Atmos. Sci.*, 1978, **35**, 714.
22. Krishnamurthy, B. V., Indukumar, S., Reddi, C. R., Raghavarao, R. and Rama, G. V., *Indian J. Radio Space Phys.*, 1986, **15**, 125.
23. Raghavarao, R., Suhasini, R., Sridharan, R., Krishnamurthy, B V. and Nagpal, O. P., *Proc. Indian Acad. Sci.*, 1990, **99**, 413.
24. Elliott, D., ed., *Handbook of Digital Signal Processing, Engineering Applications*, Academic Press, New York, 1987, pp. 602–604.
25. Houze, R. A., Jr., *J. Meteorol. Soc. Jpn.*, 1982, **60**, 396.
26. Chang, C. P., *J. Atmos. Sci.*, 1976, **33**, 740.
27. Holton, J. R., *J. Atmos. Sci.*, 1972, **29**, 368.
28. Holton, J. R., *J. Atmos. Sci.*, 1973, **30**, 499.
29. Mukherjee, B. K., Reddy, R. S. and Ramana Murthy, Bh. V., *Mon. Wea. Rev.*, 1979, **107**, 1581.
30. Mukherjee, B. K., Indira, K., Reddy, R. S. and Ramana Murthy, Bh. V., *Mon. Wea Rev.*, 1985, **113**, 1421.

ACKNOWLEDGEMENTS. We are indebted to Prof. U. R. Rao, Chairman, Indian Space Commission and Shri M. G. Chandrasekhar, Scientific Secretary, Indian Space Research Organisation (ISRO) for constant encouragement and support. The rainfall data supplied by India Meteorological Department (IMD) is thankfully acknowledged. The M-100 rocket data has been obtained from the Space Science Data Centre (SSDC), ISRO HQ, Bangalore.

Received 31 January 1992; revised accepted 15 May 1992